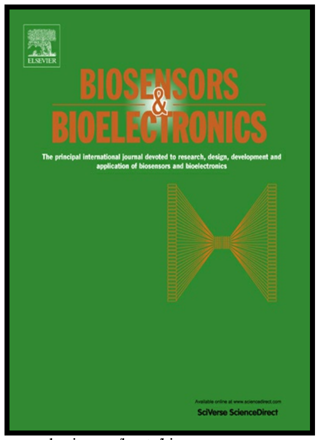

www.elsevier.com/locate/bios

Label-free nano-biosensing on the road to tuberculosis detection

Behrouz Golichenari, Kelly Velonia, Rahim Nosrati, Alireza Nezami, Aref Farokhi-Fard, Khalil Abnous, Javad Behravan, Aristidis M. Tsatsakis

PII: S0956-5663(18)30326-9
DOI: https://doi.org/10.1016/j.bios.2018.04.059
Reference: BIOS10455

To appear in: *Biosensors and Bioelectronic*

Received date: 5 February 2018
Revised date: 14 April 2018
Accepted date: 28 April 2018

Cite this article as: Behrouz Golichenari, Kelly Velonia, Rahim Nosrati, Alireza Nezami, Aref Farokhi-Fard, Khalil Abnous, Javad Behravan and Aristidis M. Tsatsakis, Label-free nano-biosensing on the road to tuberculosis detection, *Biosensors and Bioelectronic,* https://doi.org/10.1016/j.bios.2018.04.059

Label-free nano-biosensing on the road to tuberculosis detection

Behrouz Golichenari[1, 2], Kelly Velonia[3*], Rahim Nosrati[2], Alireza Nezami[4], Aref Farokhi-Fard[5], Khalil Abnous[6], Javad Behravan[1, 2]*, Aristidis M. Tsatsakis[7]

[1]. Biotechnology Research Center, Pharmaceutical Technology Institute, Mashhad University of Medical Sciences, Mashhad, Iran
[2]. Department of Pharmaceutical Biotechnology, School of Pharmacy, Mashhad University of Medical Sciences, Mashhad, Iran
[3]. Department of Materials Science and Technology, School of Sciences and Engineering, University of Crete, University Campus Voutes, 71003 Heraklion, Crete, Greece
[4]. Department of Pharmacodynamy and Toxicology, School of Pharmacy, Mashhad University of Medical Sciences, Mashhad, Iran
[5]. Biotechnology Research Center, Pasteur Institute of Iran, Tehran, Iran
[6]. Pharmaceutical Research Center, Pharmaceutical Technology Institute, Mashhad University of Medical Sciences, Mashhad, Iran
[7]. Laboratory of Toxicology, Medical School, University of Crete, Voutes, Heraklion Crete 71003, Greece
velonia@materials.uoc.gr
BehravanJ@mums.ac.ir

* Corresponding author

Abstract

Tuberculosis, an ailment caused by the bacterium *Mycobacterium tuberculosis* (*Mtb*) complex, is one of the catastrophic transmittable diseases that affect human. Reports published by WHO indicate that in 2017 about 6.3 million people progressed to TB and 53 million TB patients died from 2000 to 2016. Therefore, early diagnosis of the disease is of great importance for global health care programs. Common diagnostics like the traditional PPD test and antibody-assisted assays suffer the lack of sensitivity, long processing time and cumbersome post-test proceedings. These shortcomings restrict their use and encourage innovations in TB diagnostics. In recent years, the biosensor concept opened up new horizons in sensitive and fast detection of the disease, reducing the interval time between sampling and diagnostic result. Among new diagnostics, label-free nano-biosensors are highly promising for sensitive and accessible detection of tuberculosis. Various specific label-free nano-biosensors have been recently reported detecting the whole cell of *M. tuberculosis*, mycobacterial proteins and IFN-γ as crucial markers in early diagnosis of TB. This article provides a focused overview on nanomaterial-based label-free biosensors for tuberculosis detection.

Keywords: Label-free, Nanosensor, Surface Plasmon Resonance, Piezoelectric, Biosensor, *Mycobacterium tuberculosis*

1. Introduction

Fast detection and characterization of pathogens is of utmost consideration in human health care as some pathogens may cause disastrous diseases and conditions that affect people lives. Moreover, it is crucial for the administration of tailored antimicrobial treatment to control the spread of the disease and at the same time reduce drug resistances (Gopinath et al. 2014). Tuberculosis (TB), one of the most catastrophic phenomena that human history ever encountered, is a bacterial disease caused by transmission of one member of the *Mycobacterium tuberculosis* complex (MTBC) bacteria by different means (mostly via infected aerosols) (Comas et al. 2013; Faddoul 2015). In the 2017 global tuberculosis report, World Health Organization (WHO) estimated that 6.3 million people had developed TB and 53 million people perished due to the disease from 2000 to 2016. The report also indicates that in 2015 about 83 percent of the 5.9 million newly diagnosed and relapsed patients were treated through effective diagnosis and management (Organization 2017). Almost 70% of *Mtb*-exposed individuals are cleared from the bacteria without being infected, whereas the remaining 30 % develop the disease. In approximately 90% of infected patients, *M. tuberculosis* is either destroyed by the immune response or remains viable but functionally inactive (in dormant state) in the host macrophages. People infected with the dormant form of *Mtb* are proposed as latent TB infection (LTBI) and are considered nonclinical TB cases. It is estimated that 5 to 10 % of LTBI cases progress toward active TB, a process called "TB reactivation" (Cayabyab et al. 2012). Current diagnosis of LTBI is performed by reactive tuberculin skin testing (TST) and/or interferon-gamma release assays (IGRAs) methods (Salgame et al. 2015). Among the most fortified fortresses in the TB diagnosis to date, PCR-based, culture-colony counting and antigen–antibody interaction methods are the most frequently used protocols (Lazcka et al. 2007). Acid fast staining of sputum smear followed by microscopic assessment, despite its poor sensitivity (about 70 %), remains the most frequently exploited microbiological method for TB detection (Dorman 2010). Robert Koch introduced TST, the first and now widely available diagnostic test to an asymptomatic person exposed to tuberculosis with no clinical or radiographic signs of active TB. TST reflects a cutaneous delayed-typed hypersensitivity response to the tuberculin purified protein derivative (PPD), a complex of more than 200 *M. tuberculosis* proteins. However, it has a poor specificity in persons vaccinated with Bacille Calmette-Guérin (BCG) (since the antigens that exist in PPD cross-react with BCG and other environmental mycobacteria). It has also a low sensitivity in people with a suppressed cellular immunity (such as HIV, iatrogenic immunosuppression and children), and suffers from several other pivotal drawbacks (Lalvani 2007; Lalvani and Pareek 2009). The native PCR method cannot distinguish live from dead cells, however, the reverse transcriptase PCR method (RT-PCR) can specifically discriminate viable cells. Real-time PCR on the other hand provides faster results as it eliminates post-procedure operations such as electrophoretic molecular tracing. Culture-based methods are excessively time-consuming, requiring complicated media and need laboratory infrastructure not easily available in most of the countries bearing high burden of TB. However, they still remain a gold standard in the detection of TB. Table 1 summarizes different commercially introduced methods for TB and drug susceptibility detection up to now (Pantoja et al. 2013). The use of biosensors on the other hand, reduces the interval between sampling and obtaining the result and increases sensitivity (Lazcka et al. 2007). Considering all reasoning mentioned above, we review here the most recent research advances in the field of nano-based label-free biosensors developed for *Mtb* detection.

2. Label-free biosensors at a glance

Based on the IUPAC definition "A biosensor is a self-contained integrated device that is capable of providing specific semi-quantitative or quantitative analytical information by using biological recognition element that is in direct spatial contact with a transducer element" (Yang et al. 2010). In a biosensing module, chemical or biological events can be detected, measured and transduced in a living environment by means of a specific biorecognition element (receptor) whose features change upon binding the compound of interest and these changes are converted into a detectable signal (Ferreira et al. 2009; Nayak et al. 2009). There are several types of physicochemical transducers providing an optical (like surface plasmon resonance), piezoelectric (quartz crystal microbalance), electrochemical, thermometric, magnetic or micromechanical signal. Electrochemical biosensors are the most commercialized and accessible ones and are constructed based on amperometric, conductometric, potentiometric and impedimetric principles (Bakaltcheva et al. 1998; Gerard et al. 2002; Luo and Davis 2013).

Generally, technical strategies involved in biosensors design can be broadly divided into label-free and label-based detection (Amouzadeh Tabrizi et al. 2015). In the label-free modules, the response of analyte binding to the biorecognition element can be achieved without the use of any radioactive or fluorescent labels or any colorimetric enzymatic assays (Homola 2003). Therefore, in comparison with label-based systems, label-free biosensors have no need for high quantities of costly reagents and labels to render them a cost-effective diagnosis method for TB. Label-free biosensors in fact, are becoming a consolidated detection approach because of the direct, real-time and improved multiplexed detection capabilities they offer (Fan et al. 2008; Zanchetta et al. 2017). Recently, more sophisticated, biosensing techniques involving label-free assays promote and amplify signal through SPR (surface plasmon resonance), QCM (quartz crystal microbalance), piezoelectric, colorimetric biosensors, mass spectroscopy, and micro cantilever sensors (Cooper and Singleton 2007; Gauglitz 2010). In comparison with other biosensing methods applied for the detection of TB, such as electrochemical or fluorescence-based methods, label-free assays offer several advantages. The, mostly readable with the naked eye, colorimetric assays offer the advantage of stable performance over a varied range of time and temperatures while being commercially available for applicability in the lab as paper-based tests. In electrochemical biosensors for TB detection on the other hand, limited control on the working electrode surface at higher currents and false positive results due to the presence of electrolytes in the samples, are probably the most pronounced impediments.

Nowadays, hybrid nanomaterials (NMs) based biosensors provide nanobiosensors with synergetic properties and functions that are broadly utilized to detect and amplify biorecognition events (de la Escosura-Muñiz et al. 2010). The unique chemical and physical properties of NMs and nanoparticles (NPs), such as their intrinsic large surface area, improve biosensor performance in terms of sensitivity and selectivity, offering at the same time long shelf life (Ezzati Nazhad Dolatabadi and de la Guardia 2014).

2. 1. Surface Plasmon Resonance biosensors

SPR biosensors can detect minute amounts of analytes in complex mixtures of fluids without any requirement for prior sample preparation. SPR offers the inherent advantages of a high-throughput, real-time, noninvasive and label-free technique for the detection and monitoring of binding kinetics and affinity constants of biomolecular interactions (Chaubey and Malhotra 2002; Cosnier et al. 2002). SPR biosensors detect the SPR phenomenon expressed by the reduction in incident plane-polarized light intensity. Briefly, when a biomolecular interaction takes place on gold thin film, the refractive index in the vicinity of the surface is altered. This shift of refractive index can can be monitored by a detector (like a CCD sensor) and depicted in a sensogram (Figure 1) (Dudak and Boyacı 2009; Kausaite et al. 2007; Liedberg et al. 1983; Shankaran et al. 2007). In the recent few years, several SPR biosensors have been employed to assess protein-protein/DNA interactions in the area of *Mtb* (Barik et al. 2010; Bhattacharya et al. 2010; de Jonge et al. 2007; Dziadek et al. 2002; Elass et al. 2007; Esposito et al. 2011; Gui et al. 2011; Haagsma et al. 2011; Hegde et al. 2005; Liu et al. 2004; Mir et al. 2011; Saini et al. 2004; Schumann et al. 2006; Sengupta et al. 2006; Sidobre et al. 2002; Thakur et al. 2007; Thakur et al. 2010; Yang et al. 2010), such as biosensors involving nucleoid-associated proteins (NAPs) like Lsr2 (Leprosy serum reactive clone 2) contributing in TB drug resistance (Chen et al. 2008; Dorman and Deighan 2003; Gordon et al. 2010; Liu and Gordon 2012).

Many investigations have also been carried out to monitor *Mtb* antigens like CFP-10, the culture filtrate protein of *Mtb*, in an SPR-based detection system. Among numerous TB antigens, CFP-10 has the strongest interaction with its cognate antibody. CFP-10, is not present in the BCG vaccine strain and most nontuberculous mycobacteria, and is used as one of two main antigens in interferon gamma release-based assays. Injection of the antigen to an SPR immunosensor developed by immobilizing anti-CFP-10 antibodies enhanced SPR which returned to the baseline signal once rinsed with PBS. The limit of detection (LOD) for CFP-10 has been shown to be 100 ng mL^{-1}, with a linear relationship from 100 ng mL^{-1} to 1µg mL^{-1} (Hong et al. 2011a). The fact that most of the traditional TB diagnostics deal with the sputum or blood of TB patients may cause further increase in the risk of TB among health care professionals. Hence, Hong *et al*. designed a highly sensitive SPR system to detect CFP-10 in clinical urine samples. The detection range was from 0.1 to 1 µg mL^{-1}. However, SPR responses of healthy people that were not TB carriers showed an average peak shift of 13.8±3.67 RU that represents adsorption of unknown moieties on the gold surface and necessitates refinement of surface treatment procedures (Hong et al. 2011b). CFP-10 has also been tested in a sandwich SPR immunosensor platform using primary and secondary antibodies immobilized on nickel oxide (NiO). The dynamic range varied from 0.1 to around 150 ng mL^{-1} of CFP-10 and a detection limit as low as 0.1 ng mL^{-1} was observed (Chen et al. 2013).

SPR-based biosensing has also been used for detection of MTBC and *Mycobacterium gordonae* using thiolated single-strand oligodeoxynucleotide probes (ssODNs) immobilized on a gold-coated sensor surface. The ssODNs were complementary to specific genes in the internal transcribed spacer (ITS) sequence of both MTBC and *M. gordonae* and the resulting SPR was found to detect specific DNA hybridization at concentrations in the range of 0.05 µM, with a significant detection limit of 30 ng μL^{-1} and detection time of only 20 minutes (Duman and Piskin 2010). *M. gordonae* is not categorized as a pathogen and rarely leads to pulmonary disease (Roth et al. 2000). However, since *M. gordonae* is often present in hospital water or other environments it may cause contamination and contribute to false positive results in conventional TB detections. The strength of the aforementioned study was based on a simple sensor re-preparation protocol involving thorough rinsing with a 2.5 mM HCl solution which allowed for the sensor to be reused several times without any loss in signal intensity (Duman and Piskin 2010). Recently, an optical DNA sensor based on asymmetric isothermal amplification coupled to a silicon photonics microring sensor (SPMS-AIA) was also reported. The newly developed platform was rapid with a turnaround time of only one hour however it achieved a lower LOD (5 fg/µL) when compared with to the described SPR DNA-sensor (Liu et al. 2018). Previously, Prabhakar and colleagues (Prabhakar et al. 2008) also implemented the same nucleic acid-based platform to sense the *Mtb* genome. They used a cysteine modified NH_2-end peptide nucleic acid (PNA) probe, and 5'-thiol end labeled DNA probes immobilized on an Au coated glass electrode. PNA consists of a N-(2-aminoethyl) glycine polyamide back bone backbone wherein bases of nucleic acids are attached by a carboxymethyl moiety to the central secondary amine (Ørum et al. 1997). Self-assembled monolayers (SAMs) of thiolated DNA probes on gold usually tend to provide a formless globular configuration, while the strong electrostatic forces reduce their bioactivity. PNAs as charge-less nucleic acid analogues, provide an excellent alternative because of their increased specificity to complementary DNA and the increased stability of the PNA–DNA duplexes as compared to that of the DNA–DNA duplexes. Moreover, since PNAs have synthetic peptide-based structures, they do not have a predisposition to nuclease-mediated digestion (Metaferia et al. 2013). This was also manifested in the previous study as the PNA/Au probe had a more desirable detection limit (1.0 ng mL^{-1}) over the DNA/Au probe (3.0 ng mL^{-1}) while the PNA/Au electrode was also found to be more efficient for the detection of one-base mismatch sequences (Prabhakar et al. 2008).

Regarding single-base mismatch characterization, SPR biosensors could also be used to determine the antimicrobial resistance profile of *Mtb*, as applied in mutated *rpoB* genes. More specifically, it was demonstrated the probe and single-base mismatched target oligonucleotide form duplexes that could be detected through SPR (Rachkov et al. 2011). On the other hand, it was feasible to place the *Mtb* antigens, on a SPR sensor surface and simultaneously monitor multiple *Mtb* antibodies in serum. To achieve this, nine *Mtb* antigens were immobilized on the surface of an electrode and antibody presence against each of them was examined with an array-based SPR system. SPR response curve analysis showed serum sample of TB patients caused an initial signal increase, followed by a stabilization of the signal response. This sample caused a significant reflectivity response (R>0.6), revealing the presence of a specific antibody against this antigen in the patient-derived serum. Lower reflectivities, 0.2 to 0.5 were observed when healthy donors' samples were used. This multiplexed profile could also be compared with multiplex enzyme-linked immunosorbent assay (ELISA) assays against the same antigens. It was demonstrated that the specificity of the multiplex SPR sensor was 93% to 100%, while a range of 14% to 79% was achieved for the sensitivity. Similar experiments with the ELISA test resulted in specificity from 79% to 100% and a significantly lower sensitivity (10% to 62%) (Hsieh et al. 2012). Generally, the use of a combination of antigens for TB diagnosis is superior to the single antigen-based assay. Compared to single antigen schemes, the specificity and sensitivity of multiple-antigen strategies for SPR and ELISA systems are higher and more reliable (Houghton et al. 2002; Moran et al. 2001). Recently, a portable SPR biosensor integrated with a nested PCR technique was proposed for the rapid screening of MTBC with LOD 63 pg/mL for MTBC PCR products. Interestingly, this biosensor could successfully differentiate MTBC from other nontuberculous mycobacterium strains (Prabowo et al. 2018). The linearity range and LOD of some SPR systems for diagnosis of *M. tuberculosis* are summarized in Table 2.

Localized surface plasmon resonance (LSPR) biosensors have recently drawn much attention for point-of-care diagnosis of MTB. When compared to SPR, the LSPR systems have the advantages of simpler and more compact setups. Nanoparticles can enhance the sensitivity of LSPR biosensors when applied very close to the LSPR substrate and induce significant shifts in the LSPR peak position. In a recent study, DNA aptamers and gold nanorods (Au NRs) were utilized to create LSPR platforms and successfully detect 0.1 nM IFN-γ, a biomarker related to the diagnosis of latent tuberculosis infection (Chuang et al. 2015). In another study, a biosensor based on LSPR was developed to detect the antibody of *M. tuberculosis* using the fusion protein CFP10-ESAT6 as an antigen. In this platform, the CFP10-ESAT6 was immobilized on Au NRs, and the functionalized Au NRs were subsequently incubated with serums collected from TB patients, non-tuberculous pulmonary disease patients or healthy individuals. The change in the LSPR properties of Au NRs stemming form the specific interaction between the antigen and the target antibody was monitored. Serum analysis showed that the sensitivity of the biosensor was 79% and the specificity was 92% (Sun et al. 2017).

2. 2. Piezoelectric biosensors

Piezoelectric biosensors are considered as mass measurement devices which rely on detecting the change of resonance frequency on a quartz crystal microbalance. When an alternating electrical field is applied across the crystal, by mass binding to the electrode, it results in a change in the oscillation frequency of the QCM device. The use of QCM allows for the detection of pathogens using probes modified with immobilized antibodies. Quartz crystals are amongst the most common and popular type of materials used in piezoelectric-based platforms known as quartz crystal microbalance (Cooper 2003; Deakin and Buttry 1989; Tombelli et al. 2005). Figure 2 demonstrates a typical QCM immunosensor.

Piezoelectric quartz crystals (PQC) are crystal wafer slices sandwiched between two metal electrodes (gold or silver) created by thermal evaporation onto the quartz slice surfaces. An early TB detection piezo-immunosensor platform was developed to analyze the presence of *Mtb* in vapor aerosols (i.e. breath content) (Neuman et al. 1995). He and collaborators developed a selective and sensitive piezoelectric immunosensor detecting *Mtb* by coating protein A of *Staphylococcus aureus* onto a silver-coated PQC, to prevent nonspecific response (He and Zhang 2002). In a different study (He et al. 2002), a Thickness Shear Mode (TSM) immunosensor using a styrene-butadiene-styrene (SBS) copolymer-coated quartz crystal surface to immobilize the antibodies was evaluated. This approach resulted in accurate outputs while it was also characterized by reusability (up to six times) when washed with 4 M KSCN. Although these piezosensors are simple in design and construction, their sensitivity (about 10^5 cells mL^{-1}) is quite low and the antibodies utilized for their construction are expensive and hard to manipulate. For these reasons, He and collaborators proposed the use of a bulk acoustic wave impedance biosensor for quantitative determination of *Mtb* (He et al. 2003). This biosensor takes advantages of changes of the conductivity of the medium in which *Mtb* grows which may be traced via a frequency response curve. In this curve, the time at which the frequency starts to change is defined as Frequency Detection Time (FDT). It was found that FDT is proportional to the logarithm of the initial cell concentration of *Mtb* in the range from 2×10^3 to 3×10^7 cells mL^{-1} and can therefore be used for quantification. This platform proved to be rapid, simple, cheap and had better sensitivity (detection limit of 2×10^3 cells mL^{-1}) than the aforementioned biosensors (He et al. 2003). A stable and reusable sensor was also produced by placing protein A onto a silver-coated PQC sensor, and restricting nonspecific binding by using the irrelevant to TB, antibody-rabbit anti-honey bee venom (anti-HBV) (He and Zhang 2002). Upon specific binding of anti-TB antibodies to the bacilli, frequency shift changes were observed in the typical frequency curve over time. Detection range was 10^5 cells mL^{-1} to 10^8 cells mL^{-1} with LOD of 10^5 cells mL^{-1}, which was more sensitive compared to methods like ELISA (He and Zhang 2002). The detection of a 38 kDa protein secreted from *Mtb* using specific monoclonal antibodies Myc-31 to create a piezoelectric immunosensor showed improved detection limit than ELISA detection (Montoya et al. 2016).

A PQC biosensor constructed via immobilizing a 3-mercaptopropionic acid (MPA)/avidin/biotinylated DNA probe on a gold surface has been designed complementary to hybridize *Mtb* specific *IS6110* genomic digestions (Kaewphinit et al. 2010a, b). Since, generally, genomic DNA targeting by PQC has low possibility to complement with a DNA probe, due to the steric hindrance effect of the DNA secondary structure and the low number of copies of the target gene, the biosensor was initially tested with *IS6110*-genomic DNA digestions. The detection limit in this study was 0.5 µg mL^{-1} and a frequency shift of 78±3.4 Hz was observed. When comparing the designed biosensing test to a traditional PCR assay based on primers specific for the *IS6110* gene within sputum samples, both methods were found to possess the same sensitivity in detection however, the PQC-based method was judged to be advantageous since it is cheaper, faster, label-free and does not need to toxic substances like ethidium bromide (Kaewphinit et al. 2010a, b). Additionally, *IS6110* may primarily be amplified and tagged with gold nanoparticles (AuNPs) to further improve detection limits (Kaewphinit et al. 2012). A QCM biosensor claiming to detect whole *Mtb* and its LAM antigen in a rapid and real-time manner of less than 20 minutes, has been created using protein A-immobilized anti-H37Rv LAM rabbit polyclonal antibody (α-LAM) and anti-H37Rv whole cell guinea pig polyclonal antibody (anti-H37Rv). Minimum detection for this biosensor was 8.7×10^5 cells mL^{-1} for α-LAM and 8.7×10^6 cells mL^{-1} for anti-H37Rv (Hiatt and Cliffel 2012). Sensitive PQC-based biosensing can also be relevant to the type of crystal transducer, as detection of the 38 kDa *Mtb* antigen using 10 MHz piezoelectric crystals led to unsatisfactory results while high frequency crystals (more than 100 MHz) were required to achieve the desired detection limits (Jaramillo et al. 2014).

Ren *et al*. (Ren et al. 2008) introduced a novel multi-channel series piezoelectric quartz crystal (MSPQC) sensor for rapid detection and monitoring the volatile metabolic products of *Mtb* (NH_3 and CO_2) during growth. The series piezoelectric crystal quartz sensors are PQC sensors constructed by a series of electrodes immersed in a liquid in an oscillating circuit possessed the advantage of detecting minute changes in conductivity (Zhou et al. 2011). Diffusion of metabolites from the culture medium into a KOH absorbing solution placed beneath, resulted in changes of the conductance of the absorbing solution that were subsequently detected by the MSPQC sensor. LOD was found to be as low as 10 colony forming units (cfu). mL^{-1} and FDT exhibited a linear relationship in the range from 10^2 to 10^7 cfu mL^{-1} with the logarithm of its initial concentration. Although this method is rapid, cheap and remarkably sensitive, it requires special media such as the improved Youmans medium. In comparison to commercially available tests such as BACTEC™ MGIT™ 960 (Becton Dickinson, Sparks, MD, USA), it was shown that both methods had same accuracy in detection of the bacilli (detection limit of 10 cfu mL^{-1} for both systems), but the developed MSPQC sensor is more rapid as its FDT was shorter at the same initial concentration. In addition, the MSPQC sensor platform is prominently cheaper than the commercial sensor. In another report, a novel indirect series piezoelectric (ISP) method also based on detection of the bacilli metabolic products was introduced to detect drug-resistant *Mtb* (Ren et al. 2013). In this method, the detection relied on the propagation of 1% of an *Mtb* inoculum in drug-containing chambers as compared to that of a drug-free chamber. When sufficient amounts of drugs were added into the culture chambers, the growth of drug-sensitive *Mtb* was affected and the quantification detection time *QDT* obtained from the frequency shift change profile was found to be characteristic of *M. tuberculosis* resistance. When the *QDT* of a drug-containing chamber was found to be shorter than the *QDT* of the drug-free chamber (QDT_t), then an inoculum of *Mtb* greater than 1% growth tuberculosis was determined and the isolate was considered resistant to that special drug. When comparing sensing for three independent methods, namely the ISP system, the Agar Proportion Method (APM) and the commercial BACTEC™ MGIT™ 960 system, the mean detection time was found to be 111.7±728.45 hours, 600.0±750.30 hours and 140.3±739.52 hours, respectively, while the detection sensitivity was found to be 10-10^2 cfu mL^{-1} for all methods. It is interesting to note that the ISP sensor-based detection was found to be more cost effective.

M. smegmatis is a fast-growing mycobacterium and therefore phage amplification methods can be operated faster than the *Mtb* drug-resistant detection methods evaluating for example minimum inhibitory concentration (MIC) and APM to detect *M. tuberculosis* directly. Hence, it seems feasible to involve mycobacteriophages in sensor-assisted TB detection. Mycobacteriophages are DNA viruses that specifically infect mycobacteria, replicate, lyse the bacilli cell wall and release their progeny phage (Hatfull 2010). Mi and co-workers coupled an MSPQC sensor with the mycobacteriophage *D29* infection cycle to realize a phage amplified multi-channel series piezoelectric quartz crystal sensor (PA-MSPQC) for *Mtb* detection (Mi et al. 2011). In this platform, phage *D29* initially infected *Mtb* and in a subsequent step, the phages that remained outside *Mtb* were inactivated by ferrous ammonium sulfate (FAS) while the ones inside *Mtb* remained active. By adding the solution to the detection medium containing *M. smegmatis*, the bacillus was infected with phage *D29* imported from *Mtb* resulting in restricted *M. smegmatis* growth. Eventually, the growth response curve for *M. smegmatis* was acquired by the MSPQC system and compared to normal growth of this organism (Figure 3A). This system proved to be rapid, specific, safe and cheap. A similar platform was used to assess drug susceptibility testing of *Mtb* (Mi et al. 2014), using the same steps except pretreatment of *Mtb* with appropriate anti-mycobacterial drugs. Surviving cells were infected with phage *D29* and were involved in the subsequent steps (Figure 3B and C). More specifically, *M. smegmatis* consumed medium ingredients to grow, leading to medium conductivity change, which was monitored by the MSPQC sensor. Therefore, the growth level of *M. smegmatis* was interpreted proportional to the concentration of *M. tuberculosis*. Based on the CLSI (Clinical & Laboratory Standards Institute) criterion, the 10^5 cfu of strains with frequency shift less than 121 Hz is regarded as resistant to isoniazid, ethambutol and rifampin, while when the shift was less than 92 Hz the strain is regarded as streptomycin-resistant. Examination of drug susceptibility of 557 *Mtb* isolates by both the proposed method and by mycobacteria growth indicator tube (MGIT) led to same results (sensitivity and specificity of 91% and 93% respectively) whereas the detection time was shortened significantly (from 110 hours required for MGIT to 35 hours needed for the proposed method). In a modified version of this sensor, the steel electrode of the MSPQC system was replaced by an interdigital gold electrode to create a more sensitive IDE–SPQC sensor (He et al. 2012). In this platform, the lytic phage *D29* was immobilized on the surface of a gold electrode as probe, and *M. smegmatis* lysis following capture by immobilized phages caused a change in the electrical properties of the electrode that was monitored by the sensor. A detection limit of 10^3 cfu mL^{-1} was achieved for *M. smegmatis*, with a detection time of less than 2 hours. It is worth noting that the MSPQC sensor requires at least 250 hours for detection due to the slow growing nature of *Mtb*, while in the IDE–SPQC sensor detection can be achieved within 2 hours or less, as a result of the short time of adsorption and lysis and the simpler detection medium used. Based on the detection of the specific fused antigen CFP10-ESAT6, another IDE-MSPQC sensor was constructed using the CFP10-ESAT6 aptamer as specific probe to attain MTB detection at 96.3h (He et al. 2016). The linearity range and LOD of some piezoelectric platforms for diagnosis of *M. tuberculosis* are summarized in Table 2.

2. 3. Gold nanoparticle-based colorimetric approaches

The smart control recently obtained over the extraordinary properties of nano-scaled materials has created unique prospects for their incorporation in a wide field of point-of-care diagnostics. While most traditional methods require complicated, time-consuming and high-cost instruments that limit their use, colorimetric biosensors are coupled to reactions that lead to creating a visible color and can often be considered more convenient and rapid since changes can be observed even by naked eye (Lee et al. 2006; Wang et al. 2010). Colorimetric detectors are mostly characterized by simplicity in operation and lack of need for complicated or expensive instruments. These characteristics combined with the high absorption coefficients (often 1000 times greater than those of organic dyes) and excellent shape, size and distance dependent optical properties arising from the SPR effect render AuNPs as first line components for the development of colorimetric detection systems (Baptista et al. 2008; Liandris et al. 2009; Mirkin et al. 1996; Syed and Bokhari 2011; Yang et al. 2011; Zhao et al. 2007). In such systems, AuNPs can be functionalized with antibodies or other ligands such as thiol modified ssDNA or PNA sequences (due to increased stability and mismatch sensitivity) (Teengam et al. 2017), complementary to pathogen-raised DNA or RNAs. In fact, building on the platform first described by Mirkin and co-workers (Mirkin et al. 1996), nucleotide probes conjugated with gold nanoparticles (AuNP-probes) have been extensively utilized for mycobacterial DNA characterization in different samples. After introduction of salt (NaCl or $MgCl_2$) or acids like HCl, in the absence of the complementary target (also in the case of non-complementary or mismatched sequences), the ssDNA probes are absorbed on the AuNPs surface, protect them from aggregation and the solution remains red (~526 nm). However, in the presence of target DNA hybridizing to probe on the surface of the functionalized AuNPs and facilitating inter-particle crosslinking and aggregation, the color visibly turns from red to purple (around 600 nm) (Figure 4) (Baptista et al. 2008; Liandris et al. 2009; Mirkin et al. 1996; Syed and Bokhari 2011). In another approach, absence of a target sequence induced aggregation of anion-stabilized silver nanoparticles (AgNPs) while, the presence of a target DNA dispersion of the nanoparticles gave rise to a detectable color change (Teengam et al. 2017). In addition to simplicity and low-cost, gold nanoparticle-based assays have also demonstrated more sensitivity than Ziehl–Neelsen (ZN) acid-fast smear examination (Baptista et al. 2006) and the PCR (Upadhyay et al. 2006) *Mtb* detection from various clinical specimens. In an ordinary Au-nanoprobe system, an amplification process like conventional PCR (Soo et al. 2009; Upadhyay et al. 2006), nested-PCR (Hussain 2011), nucleic acid sequence-based amplification (NASBA) (Gill et al. 2008), loop-mediated isothermal amplification (LAMP) (Kaewphinit et al. 2013; Veigas et al. 2013), rolling circle amplification (RCA) (Pavankumar et al. 2016) and recombinase polymerase amplification (RPA) (Chuang et al. 2015), is primarily utilized to multiply the number of mycobacterial target sequence copies. It is important to note that in the AuNP detection systems this can be achieved without any pre-amplification (Liandris et al. 2009). Various mycobacterial genomic regions like IS*6110* (Soo et al. 2006; Upadhyay et al. 2006), 16s rDNA (Hussain et al. 2013), *rpoB* (Baptista et al. 2006), *katG* (Pavankumar et al. 2016) and *gyrB* (Costa et al. 2010) genes have been targeted to hybridization with such probes.

In order to improve sensitivity of detection, a combination of multiplex nested PCR with immuno-chromatography test (ICT) has led to high specific amplification of mycobacterial genomic DNA and observation of a positive color response. For the detection of MTBC, 95.5% sensitivity and 97.9% specificity was achieved, while a 93.0% sensitivity and 99.8% specificity was obtained for *Mtb* (Soo et al. 2006). However, antibodies are expensive and therefore, using them to create a routine test may be controversial. For this reason, similar platforms were developed with AuNPs along with thiol-modified oligonucleotides. This profile significantly reduced spending costs, as no antibodies were incorporated or other labels required. More importantly, improved yields, 96.6% sensitivity and 98.9% specificity of MTBC detection and 99.6% specificity and 94.7% sensitivity for *Mtb* were achieved (Soo et al. 2009).

As previously noted, mismatches or single-nucleotide polymorphisms (SNPs) within the *Mtb* genome restrain DNA strand hybridization, which results in color formation and causes AuNPs to remain in solution. This reduced hybridization efficiency was advantageously used in mycobacterial drug-resistance determination. The gene *rpoB* encodes the β-subunit of the RNA polymerase; it has an 81 bp region (codons 507–533) that contains the SNPs, which accounts for resistance to rifampicin (RIF). A study on SNPs associated in RIF-resistance using Au-nanoprobes and the INNO-LiPA Rif. TB assay (Innogenetics, Belgium) showed 81% concordance (34 out of 42 cases) between the two methods. The lack of detection in eight samples with Au-nanoprobes was further analyzed with sequencing and attributed to other rare SNPs that have not been introduced along probes and necessitate further optimization to complete recognition of RIF-resistance possibilities (Veigas et al. 2010). Pavankumar *et al*. (Pavankumar et al. 2016) studied a padlock probe-lateral flow test (PLP-LF) in which RCA served to characterize the mutations in the *katG*315 and *rpoB*531 codons responsible for multi-drug resistance in *Mtb*. If the gene in question underwent mutation, the 5′ and 3′ arms of padlock-shape sequence would not hybridize properly and rolling circle amplification would not occur. The limit of detection was measured to be as low as 3 ng of genomic DNA for the *katG* and 30 ng for the *rpoB* gene, while 300 ng was the limit achieved for simultaneous detection of both gene mutations (Pavankumar et al. 2016). The concordance of AuNP-based colorimetry with the aforementioned real-time PCR methods was 87.5% sensitivity and 100% specificity in MTBC detection (Liandris et al. 2009). In another study, an AuNP-based protocol conjugated with pre-amplification showed a detection limit of 1 ng for the PCR product and 40 ng for genomic DNA with 100% concordance with BACTEC™ MGIT™ and semi-nested PCR which is acceptable among these trusted diagnostics (Hussain et al. 2013). Coupling the LAMP method with Au-nanoprobes was found to reduce the time of detection compared to other amplification procedures that couple with Au-nanoprobes, because of the absence of need for thermal cycling (Veigas et al. 2013). However, the preparation of AuNPs functionalized with thiol-modified ssDNAs is not only complicated and time-consuming, but further requires highly trained synthetic personnel. Interestingly to address such issues, a paper-based tuberculosis diagnostic test based on free ssDNA probes and lacking the need to use modified AuNPs was recently developed (Tsai et al. 2013). This method achieved a low detection limit of 2.6 nM for the extracted mycobacterial target sequence and a low diagnosis time that indicates it could be much more applicable than routine Au–thiol bound probe-based methods (Tsai et al. 2013).

The AuNP-based *Mtb* detection methods utilizing a conventional target DNA amplification step, require three hours from sample collection to characterization of the bacilli, two hours and 30 minutes for PCR and approximately thirty minutes for the colorimetric assay render it most promising among the options for point-of-care detection of TB (Silva et al. 2011). Kim and colleagues (Kim et al. 2013) developed a novel magnetophoretic immunoassay (MPI) that can detect CFP-10 in positive samples in only over 10 minutes. They reported that, with the use of anti-CFP-10 antibody [G2] conjugated to AuNPs, together with another anti-CFP-10 antibody [G2] conjugated to MMPs (magnetic microparticles), the AuNP-[G2] probes could be removed from a solution by magnetophoresis. In the presence of CFP-10, the plasmon absorbance of the solution decreased and red color weakened. The detection range for the assay varied from 10 to 10,000 pg mL^{-1} with a detection limit of 10 pg mL^{-1} (Kim et al. 2013). The implementation of any research-scale diagnostic procedure in a high-throughput framework is the desired goal for every lab-scale diagnostic module. With this view, a colorimetric AuNP-based platform has recently implemented within paper microplate wells. Detection of MTBC through a color change which was recorded by a camera of the generic smartphone device or other available detectors demonstrated the sensitivity and specificity of this method (Veigas et al. 2012). Integration of gold nanoprobes into a lab-on-a-chip microfluidic platform in order to miniaturize reagent and sample volumes and reduce costing was also feasible. In such a configuration, a disposable inexpensive microfluidic chip was developed that required only 3 μL of the DNA solution with a concentration of 30 ng μL^{-1} of target DNA achieving a 20-fold reduction of required solution volume as compared to the bulk version of AuNP-based biosensor (Bernacka-Wojcik et al. 2013). In fact, microfluidic channels have recently attracted much attention in POC diagnostics as they are designed to accommodate all detection constituents within micro-scale channels which reduce material consumption and handling, along with providing a low-cost, user-friendly, detection tool (Farre et al. 2012). Among label-free methods for the detection of TB, the colorimetric methods are used as a highly specific and sensitive screening tool for the detection of mycobacteria directly from clinical samples (Liandris et al. 2009).

2.4. Other label-free TB detection sensors

The microcantilever based biosensors and mass spectroscopy (MS) have also been proven to be interesting systems for tuberculosis detection. In microcantilever platforms, for the of conversion of biorecognition into nanomechanical motion, specific antibodies need to be immobilize on the cantilever surface. Once patient sample containing tuberculosis antigens is placed on the functionalized cantilever surface, a biochemical reaction between tuberculosis antigens and antibodies occurs. Adsorption of antigens, increases the mass of the operating cantilever and results in bending (stress) of the microcantilever. Murthy et al. designed and applied a microcantilever device for the detection of the TB antigen 85 complex by specific antibodies. The accuracy of the sensor was found to be high when length of 20 μm and width of 5 μm was used (Murthy et al. 2016). Microelectromechanical systems (MEMS)/nanoelectromechanical systems are also used for designing such biosensors to identify a presence of TB in a suspected patient's blood (Rao and Jasti 2016; Saeed et al. 2016). EMS are tiny micromachined systems that are typically arranged on small chips for different purposes. Using such MEMS biosensors, tuberculosis can be identified very accurately and rapidly in comparison to other existing methods. A recent study aiming at the detection of primary stages of tuberculosis was based on ESAT-6. Specific antibodies immobilized on top of a microcantilever and patient samples consisting of ESAT-6 were utilized. Upon the biochemical reaction between antigens ESAT-6 and antibodies, adsorption of antigens resulted in bending of the microcantilever which was assessed as presence of tuberculosis within the patient sample (Dhakane and Patil 2014).

MS has also proven to be a potent tool for the characterization of antigenic peptides in infectious TB. MS provides highly accurate molecular weight of biomarkers and highly reproducible results. Hence, MS coupled with liquid chromatography is a powerful instrument for rapidly identifying the presence of the bacteria in biological fluids (plasma, serum, urine or tissue) (López-Hernández et al. 2016). The development of matrix-assisted laser desorption ionization time-of-flight mass spectrometry (MALDI-TOF-MS) introduced an alternative method for easy, rapid and efficient identification of micro-organisms (Lay 2001). In the past years, numerous studies utilized of MALDI-TOF-MS for accurate identification of mycobacteria. For example, Hettick et al. (2006) identified 16 mycobacterial strains. Pignone et al. (2006) reported among 37 strains of rapid and slow-growing mycobacteria, producing species-specific patterns for 36 of the isolates. Lotz et al. (2010)

used intact bacterial cells to obtain bacterial mass spectral fingerprints and verified that this technique could be easily performed in routine clinical laboratories by any operator in a few minutes. Shitikov et al. (2012) analyzed 383 clinical isolates by MALDI-TOF-MS and obtained 342 strains of MTB, 6 strains of *M. bovis* and 35 strains of non-tuberculous mycobacteria belonging to 16 different species. In another study, six strains of *M. tuberculosis*, such as 16S rDNA, rpoB and hsp65, were differentiated using MALDI-TOF-MS with higher resolution than with other techniques (Wang et al. 2012). Saleeb et al. (2011) developed a protein extraction protocol specifically designed for *mycobacteria*. In this work, the timeline from sample preparation to results was approximately 90 min. More recently, Tudo et al. (2015) used MALDI-TOF-MS for analyzing of 243 mycobacterial isolates of positive cultures and acquired all results within a few hours.

3. Conclusions and future perspectives

Given that in countries with high rates of TB cases, access to cheaper reliable diagnostics is one of the most important goals in controlling the disease, biosensors can play a critical role. This review summarized a variety of label-free biosensors designed to detect TB with a detection sensitivity in the femtomolar range for pathogen-raised biomolecules. Analysis of the works published during the last two decades revealed that combination of nanomaterial science, microfluidics (Barroso et al. 2018; Bernacka-Wojcik et al. 2013) and nucleic acid technologies (aptamers and isothermal amplification techniques) provide great prospects in the fabrication of new TB biosensing platforms with very high detection speed, sensitivity and accuracy. Considering the importance of diagnosis in the latent phase, there is still a need for developing inexpensive devices with lower detection limits for clinical and screening purposes. In this review we focused on efficient sensors using low sample volumes as compared to the routine commercialized methods. The platforms reviewed do not require labels to direct detection toward a reproducible and sensitive signal. However, it seems that many of the platforms described here are significantly more expensive than applicable in developing countries so, planning simpler designs for TB DNA sensors based for example on deoxyribozyme (Bengtson et al. 2017) or molecular beacons ("sensor with tiered output for dual targets": STODT) (Huang et al. 2017), is crucial for multiplex analysis of MDR- and XDR- TB. Sensors that do not require complex agents, functionalization or sophisticated instrumentation like the SPR sensing system can offer valuable alternatives. We anticipate that in the near future, simple portable diagnostic tools capable of multi analytes detection meeting the needs of high-prevalence areas will evolve. With these in mind, application of biosensors from bench to clinical diagnosis can pave the route to global objectives of TB control.

Acknowledgments

Funding for the laboratories of JB was provided by Mashhad University of Medical Sciences, AT and KA have.

Conflict of interests

The authors declare no conflict of interests.

References

Amouzadeh Tabrizi, M., Shamsipur, M., Farzin, L., 2015. Biosens. Bioelectron. 74, 764-769.

Bakaltcheva, I.B., Shriver-Lake, L.C., Ligler, F.S., 1998. Sens. Actuator B-Chem. 51(1), 46-51.

Baptista, P., Pereira, E., Eaton, P., Doria, G., Miranda, A., Gomes, I., Quaresma, P., Franco, R., 2008. Anal. Bioanal. Chem. 391(3), 943-950.

Baptista, P.V., Koziol-Montewka, M., Paluch-Oles, J., Doria, G., Franco, R., 2006. Clin. Chem. 52(7), 1433-1434.

Barik, S., Sureka, K., Mukherjee, P., Basu, J., Kundu, M., 2010. Mol. Microbiol. 75(3), 592-606.

Barroso, T.G., Martins, R.C., Fernandes, E., Cardoso, S., Rivas, J., Freitas, P.P., 2018. Biosens. Bioelectron. 100, 259-265.

Bengtson, H.N., Homolka, S., Niemann, S., Reis, A.J., da Silva, P.E., Gerasimova, Y.V., Kolpashchikov, D.M., Rohde, K.H., 2017. Biosens. Bioelectron. 94, 176-183.

Bernacka-Wojcik, I., Lopes, P., Vaz, A.C., Veigas, B., Wojcik, P.J., Simões, P., Barata, D., Fortunato, E., Baptista, P.V., Águas, H., 2013. Biosens. Bioelectron. 48, 87-93.

Bhattacharya, M., Biswas, A., Das, A.K., 2010. Biochim. 92(3), 263-272.

Bholla, M., Kapalata, N., Masika, E., Chande, H., Jugheli, L., Sasamalo, M., Glass, T.R., Beck, H.-P., Reither, K., 2016. BMC Infect. Dis. 16, 246.

Cayabyab, M.J., Macovei, L., Campos-Neto, A., 2012. Front Cell Infect Microbiol. 2.

Chaubey, A., Malhotra, B., 2002. Biosens. Bioelectron. 17(6), 441-456.

Chen, H., Liu, F., Koh, K., Lee, J., Ye, Z., Yin, T., Sun, L., 2013. Microchim. Acta. 180(5-6), 431-436.

Chen, J.M., Ren, H., Shaw, J.E., Wang, Y.J., Li, M., Leung, A.S., Tran, V., Berbenetz, N.M., Kocíncová, D., Yip, C.M., 2008. Nucleic Acids Res. 36(7), 2123-2135.

Chuang, P.-C., Liao, P.-C., Chen, Y.-F., 2015. Enhancing the sensitivity of localized surface plasmon resonance (LSPR) biosensors using nanorods and DNA aptamers. SPIE BiOS, p. 4. SPIE.

Cloud, J.L., Shutt, C., Aldous, W., Woods, G., 2004. J. Clin. Microbiol. 42(11), 5341-5344.

Comas, I., Coscolla, M., Luo, T., Borrell, S., Holt, K.E., Kato-Maeda, M., Parkhill, J., Malla, B., Berg, S., Thwaites, G., 2013. Nat. Genet. 45(10), 1176-1182.

Cooper, M.A., 2003. Anal. Bioanal. Chem. 377(5), 834-842.

Cooper, M.A., Singleton, V.T., 2007. J. Mol. Recognit. 20(3), 154-184.

Cosnier, S., Novoa, A., Mousty, C., Marks, R.S., 2002. Anal. Chim. Acta. 453(1), 71-79.

Costa, P., Amaro, A., Botelho, A., Inácio, J., Baptista, P.V., 2010. Clin. Microbiol. Infect. 16(9), 1464-1469.

Daghestani, H.N., Day, B.W., 2010. Sensors. 10(11), 9630-9646.

de Jonge, M.I., Pehau-Arnaudet, G., Fretz, M.M., Romain, F., Bottai, D., Brodin, P., Honoré, N., Marchal, G., Jiskoot, W., England, P., 2007. J. Bacteriol. 189(16), 6028-6034.

de la Escosura-Muñiz, A., Parolo, C., Merkoçi, A., 2010. Materials Today 13(7), 24-34.

Deakin, M.R., Buttry, D.A., 1989. Anal. Chem. 61(20), 1147A-1154A.

Dhakane, S., Patil, W.V., 2014. Microsyst. Technol. 20(3), 457-462.

Dorman, C.J., Deighan, P., 2003. Curr. Opin. Genet. Dev. 13(2), 179-184.

Dorman, S.E., 2010. Clin. Infect. Dis. 50(Supplement 3), S173-S177.

Dudak, F.C., Boyacı, İ.H., 2009. Biotechnol. j. 4(7), 1003-1011.

Duman, M., Piskin, E., 2010. Biosens. Bioelectron. 26(2), 908-912.

Dziadek, J., Rajagopalan, M., Parish, T., Kurepina, N., Greendyke, R., Kreiswirth, B.N., Madiraju, M.V., 2002. J. bacteriol. 184(14), 3848-3855.

Elass, E., Coddeville, B., Guérardel, Y., Kremer, L., Maes, E., Mazurier, J., Legrand, D., 2007. FEBS lett. 581(7), 1383-1390.

Esposito, C., Marasco, D., Delogu, G., Pedone, E., Berisio, R., 2011. Biochem. Biophys. Res. Commun. 410(2), 339-344.

Ezzati Nazhad Dolatabadi, J., de la Guardia, M., 2014. Analytical Methods 6(12), 3891-3900.

Faddoul, D., 2015. Adv. pediatrics 62(1), 59-90.

Fan, X., White, I.M., Shopova, S.I., Zhu, H., Suter, J.D., Sun, Y., 2008. Anal. Chim. Acta. 620(1-2), 8-26.

Farre, M., Kantiani, L., Barcelo, D., 2012.

Ferreira, G.N., da-Silva, A.-C., Tomé, B., 2009. Trends. Biotechnol. 27(12), 689-697.

Gauglitz, G., 2010. Anal. Bioanal. Chem. 398(6), 2363-2372.

Gerard, M., Chaubey, A., Malhotra, B., 2002. Biosens. Bioelectron. 17(5), 345-359.

Gill, P., Ghalami, M., Ghaemi, A., Mosavari, N., Abdul-Tehrani, H., Sadeghizadeh, M., 2008. Nanobiotechnology 4(1-4), 28-35.

Gopinath, S.C., Tang, T.-H., Chen, Y., Citartan, M., Lakshmipriya, T., 2014. Biosens. Bioelectron. 60, 332-342.

Gordon, B.R., Li, Y., Wang, L., Sintsova, A., van Bakel, H., Tian, S., Navarre, W.W., Xia, B., Liu, J., 2010. Proc. Natl. Acad. Sci. 107(11), 5154-5159.

Gui, W.-J., Lin, S.-Q., Chen, Y.-Y., Zhang, X.-E., Bi, L.-J., Jiang, T., 2011. Biochem. Biophys. Res. Commun. 405(2), 272-277.

Haagsma, A.C., Podasca, I., Koul, A., Andries, K., Guillemont, J., Lill, H., Bald, D., 2011. PLoS One. 6(8), e23575.

Hatfull, G.F., 2010. Annu. Rev. Microbiol. 64, 331-356.

He, F., Xiang, M., Mi, X., 2012. Anal. Lett. 45(10), 1242-1253.

He, F., Xiong, Y., Liu, J., Tong, F., Yan, D., 2016. Biosens. Bioelectron. 77, 799-804.

He, F., Zhang, L., 2002. Anal. sci. 18(4), 397-401.

He, F., Zhang, L., Zhao, J., Hu, B., Lei, J., 2002. Sens. Actuator B-Chem. 85(3), 284-290.

He, F., Zhao, J., Zhang, L., Su, X., 2003. Talanta. 59(5), 935-941.

Hegde, S.S., Vetting, M.W., Roderick, S.L., Mitchenall, L.A., Maxwell, A., Takiff, H.E., Blanchard, J.S., 2005. Science. 308(5727), 1480-1483.

Hettick, J.M., Kashon, M.L., Slaven, J.E., Ma, Y., Simpson, J.P., Siegel, P.D., Mazurek, G.N., Weissman, D.N., 2006. Proteomics. 6(24), 6416-6425.

Hiatt, L.A., Cliffel, D.E., 2012. Sens. Actuator B-Chem. 174, 245-252.

Homola, J., 2003. Anal. Bioanal. Chem. 377(3), 528-539.

Hong, S.C., Chen, H., Lee, J., Park, H.-K., Kim, Y.S., Shin, H.-C., Kim, C.-M., Park, T.J., Lee, S.J., Koh, K., 2011a. Sens. Actuator B-Chem. 156(1), 271-275.

Hong, S.C., Lee, J., Shin, H.-C., Kim, C.-M., Park, J.Y., Koh, K., Kim, H.-J., Chang, C.L., Lee, J., 2011b. Sens. Actuator B-Chem. 160(1), 1434-1438.

Houghton, R.L., Lodes, M.J., Dillon, D.C., Reynolds, L.D., Day, C.H., McNeill, P.D., Hendrickson, R.C., Skeiky, Y.A., Sampaio, D.P., Badaro, R., 2002. Clin. Diagn. Lab. Immunol. 9(4), 883-891.

Hsieh, S.-C., Chang, C.-C., Lu, C.-C., Wei, C.-F., Lin, C.-S., Lai, H.-C., Lin, C.-W., 2012. Nanoscale Res. Lett. 7(1), 1-6.

Huang, S.-Y., Chang, J.-R., Liao, Y.-C., Dou, H.-Y., Chuang, M.-C., 2017. Anal. Chim. Acta.

Hussain, M.M., 2011. Direct detection of *Mycobacterium tuberculosis* complex using gold nanoparticles. The American University in Cairo.

Hussain, M.M., Samir, T.M., Azzazy, H.M., 2013. Clin. Biochem. 46(7), 633-637.

Jaramillo, M., Marín, P., Torres, R., Pabón, E., Montagut, Y., Robledo, J., Moreno, M., Manclús, J., Montoya, A., 2014. Advances in the development of a piezoelectric immunosensor for the detection of a tuberculosis biomarker. Sensors (IBERSENSOR), 2014 IEEE 9th Ibero-American Congress on, pp. 1-4. IEEE.

Kaewphinit, T., Santiwatanakul, S., Chansiri, K., 2012. Sensors & Transducers. 146(11), 156.

Kaewphinit, T., Santiwatanakul, S., Chansiri, K., 2013. Sensors & Transducers. 149(2), 123.

Kaewphinit, T., Santiwatanakul, S., Promptmas, C., Chansiri, K., 2010a. Sensors. 10(3), 1846-1858.

Kaewphinit, T., Santiwatanakul, S., Promptmas, C., Chansiri, K., 2010b. Sensors & Transducers. 113(2), 115.

Kausaite, A., van Dijk, M., Castrop, J., Ramanaviciene, A., Baltrus, J.P., Acaite, J., Ramanavicius, A., 2007. Biochem. Mol. Biol. Educ. 35(1), 57-63.

Kim, J., Lee, J., Lee, K.-I., Park, T.J., Kim, H.-J., Lee, J., 2013. Sens. Actuator B-Chem. 177, 327-333.

Kim, J.H., Kim, Y.J., Ki, C.-S., Kim, J.-Y., Lee, N.Y., 2011. J. Clin. Microbiol. 49(1), 173-176.

Kumar Singh, A., Verma, N., 2014. Curr. Biotechnol. 3(2), 127-132.

Lalvani, A., 2007. CHEST J. 131(6), 1898-1906.

Lalvani, A., Pareek, M., 2009. Br. Med. Bull., ldp039.

Lay, J.O., 2001. Mass. Spectrom. Rev. 20(4), 172-194.

Lazcka, O., Del Campo, F.J., Munoz, F.X., 2007. Biosens. Bioelectron. 22(7), 1205-1217.

Lee, N.Y., Jung, Y.K., Park, H.G., 2006. Biochem. Eng. J. 29(1), 103-108.

Liandris, E., Gazouli, M., Andreadou, M., Čomor, M., Abazovic, N., Sechi, L.A., Ikonomopoulos, J., 2009. J. Microbiol. Methods. 78(3), 260-264.

Liedberg, B., Nylander, C., Lunström, I., 1983. Sens. actuators B-chem 4, 299-304.

Liu, C., He, Y., Chang, Z., 2004. Biochem. Biophys. Res. Commun. 316(4), 1163-1172.

Liu, J., Gordon, B.R., 2012. Expert Rev Anti Infect Ther. 10(9), 1049-1053.

Liu, Q., Lim, B.K.L., Lim, S.Y., Tang, W.Y., Gu, Z., Chung, J., Park, M.K., Barkham, T., 2018. Sens. Actuator B-Chem. 255, 1595-1603.

López‐Hernández, Y., Patiño‐Rodríguez, O., García‐Orta, S., Pinos‐Rodríguez, J., 2016. J. Appl. Microbiol. 121(6), 1485-1497.

Lotz, A., Ferroni, A., Beretti, J.-L., Dauphin, B., Carbonnelle, E., Guet-Revillet, H., Veziris, N., Heym, B., Jarlier, V., Gaillard, J.-L., 2010. J. Clin. Microbiol. 48(12), 4481-4486.

Luo, X., Davis, J.J., 2013. Chem. Soc. Rev. 42(13), 5944-5962.

Metaferia, B., Wei, J.S., Song, Y.K., Evangelista, J., Aschenbach, K., Johansson, P., Wen, X., Chen, Q., Lee, A., Hempel, H., 2013. PloS one. 8(4), e58870.

Metcalfe, J.Z., Cattamanchi, A., McCulloch, C.E., Lew, J.D., Ha, N.P., Graviss, E.A., 2013. Am J Respir Crit Care Med. 187(2), 206-211.

Mhimbira, F.A., Bholla, M., Sasamalo, M., Mukurasi, W., Hella, J.J., Jugheli, L., Reither, K., 2015. J. Clin. Microbiol. 53(4), 1342-1344.

Mi, X., He, F., Xiang, M., Lian, Y., Yi, S., 2011. Anal. chem. 84(2), 939-946.

Mi, X., He, F., Xiang, M., Lian, Y., Yi, S., 2014. Sens. Actuator B-Chem. 193, 715-722.

Mir, M., Asong, J., Li, X., Cardot, J., Boons, G.-J., Husson, R.N., 2011. PLoS pathog 7(7), e1002182.

Mirkin, C.A., Letsinger, R.L., Mucic, R.C., Storhoff, J.J., 1996. Nature. 382(6592), 607-609.

Montoya, A., March, C., Montagut, Y., Moreno, M., Manclús, J., Arnau, A., Jiménez, Y., Jaramillo, M., Marín, P., Torres, R., 2016. Curr. Top. Med. Chem.

Moran, A.J., Treit, J.D., Whitney, J.L., Abomoelak, B., Houghton, R., Skeiky, Y.A., Sampaio, D.P., Badaró, R., Nano, F.E., 2001. FEMS. Microbiol. Lett. 198(1), 31-36.

Murthy, K., Prasad, G., Saikiran, N., Manoj, T., 2016. Indian J Sci Technol. 9(31).

Nayak, M., Kotian, A., Marathe, S., Chakravortty, D., 2009. Biosens. Bioelectron. 25(4), 661-667.

Neuman, M., Perlaky, S., Michalski, J., Bass, J., McCombs, C., 1995. Detection of TB antigens in liquid and vapor phases by an antibody-based piezoelectric biosensor. Engineering in Medicine and Biology Society, 1995., IEEE 17th Annual Conference, pp. 1563-1564. IEEE.

Nguyen, V.A.T., Nguyen, H.V., Dinh, T.V., Du, H.H., Do, C.N., Marks, G.B., Nguyen, N.V., 2018. Diagn. Microbiol. Infect. Dis. 90(3), 190-195.

Nirschl, M., Reuter, F., Vörös, J., 2011. Biosensors. 1(3), 70-92.

Organization, W.H., 2017.

Ørum, H., Kessler, C., Koch, T., 1997. Peptide nucleic acid. Nucleic acid amplification technologies: application to disease diagnosis. Eaton Publishing, Natick, Mass, pp. 29-48.

Pantoja, A., Fitzpatrick, C., Vassall, A., Weyer, K., Floyd, K., 2013. Eur. Respir. J. 42(3), 708-720.

Pavankumar, A.R., Engström, A., Liu, J., Herthnek, D., Nilsson, M., 2016. Anal. chem. 88(8), 4277-4284.

Pignone, M., Greth, K.M., Cooper, J., Emerson, D., Tang, J., 2006. J. Clin. Microbiol. 44(6), 1963-1970.

Prabhakar, N., Arora, K., Arya, S.K., Solanki, P.R., Iwamoto, M., Singh, H., Malhotra, B., 2008. Analyst. 133(11), 1587-1592.

Prabowo, B.A., Chang, Y.-F., Lai, H.-C., Alom, A., Pal, P., Lee, Y.-Y., Chiu, N.-F., Hatanaka, K., Su, L.-C., Liu, K.-C., 2018. Sens. Actuator B-Chem. 254, 742-748.

Rachkov, A., Patskovsky, S., Soldatkin, A., Meunier, M., 2011. Talanta. 85(4), 2094-2099.

Rao, K.S., Jasti, S., 2016. Design and analysis of MEMS based bio sensor for TB detection. Electrical, Electronics, Communication, Computer and Optimization Techniques (ICEECCOT), 016 International Conference on, pp. 361-365. IEEE.

Ren, J., He, F., Yi, S., Cui, X., 2008. Biosens. Bioelectron. 24(3), 403-409.

Ren, J., Ma, L., Li, Z., Huang, H., Yi, S., 2013. Biosens. Bioelectron. 43, 115-119.

Roth, A., Reischl, U., Streubel, A., Naumann, L., Kroppenstedt, R.M., Habicht, M., Fischer, M., Mauch, H., 2000. J. Clin. Microbiol. 38(3), 1094-1104.

Saeed, M.A., Khan, S.M., Ahmed, N., Khan, M.U., Rehman, A., 2016. Design and analysis of capacitance based Bio-MEMS cantilever sensor for tuberculosis detection. Intelligent Systems Engineering (ICISE), 2016 International Conference on, pp. 175-180. IEEE.

Saini, A.K., Maithal, K., Chand, P., Chowdhury, S., Vohra, R., Goyal, A., Dubey, G.P., Chopra, P., Chandra, R., Tyagi, A.K., 2004. J. Biol. Chem. 279(48), 50142-50149.

Saleeb, P.G., Drake, S.K., Murray, P.R., Zelazny, A.M., 2011. J. Clin. Microbiol. 49(5), 1790-1794.

Salgame, P., Geadas, C., Collins, L., Jones-López, E., Ellner, J.J., 2015. Tuberculosis.

Schumann, G., Schleier, S., Rosenkrands, I., Nehmann, N., Hälbich, S., Zipfel, P.F., de Jonge, M.I., Cole, S.T., Munder, T., Möllmann, U., 2006. Cent Eur J Biol. 1(2), 183-202.

Sengupta, S., Shah, M., Nagaraja, V., 2006. Nucleic acids res. 34(19), 5567-5576.

Shah, M., Hanrahan, C., Wang, Z.Y., Dendukuri, N., Lawn, S.D., Denkinger, C.M., Steingart, K.R., 2016. Cochrane Database Syst Rev. (5), 1-108.

Shankaran, D.R., Gobi, K.V., Miura, N., 2007. Sens. Actuator B-Chem. 121(1), 158-177.

Sharma, A.K., Jha, R., Gupta, B., 2007. IEEE Sensors Journal 7(8), 1118-1129.

Shitikov, E., Ilina, E., Chernousova, L., Borovskaya, A., Rukin, I., Afanas'ev, M., Smirnova, T., Vorobyeva, A., Larionova, E., Andreevskaya, S., 2012. Infect. Genet. Evol. 12(4), 838-845.

Sidobre, S., Germain, P., Rivière, M., 2002. Biochem. J. 365(1), 89-97.

Silva, L.B., Veigas, B., Doria, G., Costa, P., Inácio, J., Martins, R., Fortunato, E., Baptista, P.V., 2011. Biosens. Bioelectron. 26(5), 2012-2017.

Simsek, H., Alpar, S., Uçar, N., Aksu, F., Ceyhan, I., Gozalan, A., Cesur, S., Ertek, M., 2010. Jpn J Infect Dis. 63(2), 99-102.

Skládal, P., 2003. J. Braz. Chem. Soc. 14(4), 491-502.

Soo, P.-C., Horng, Y.-T., Chang, K.-C., Wang, J.-Y., Hsueh, P.-R., Chuang, C.-Y., Lu, C.-C., Lai, H.-C., 2009. Mol. Cell. Probes. 23(5), 240-246.

Soo, P.-C., Horng, Y.-T., Hsueh, P.-R., Shen, B.-J., Wang, J.-Y., Tu, H.-H., Wei, J.-R., Hsieh, S.-C., Huang, C.-C., Lai, H.-C., 2006. J. Microbiol. Methods. 66(3), 440-448.

Sun, W., Yuan, S., Huang, H., Liu, N., Tan, Y., 2017. J. Microbiol. Methods. 142, 41-45.

Syed, M.A., Bokhari, S., 2011. J. Biomed. Nanotechnol. 7(2), 229-237.

Teengam, P., Siangproh, W., Tuantranont, A., Vilaivan, T., Chailapakul, O., Henry, C.S., 2017. Anal. Chem. 89(10), 5428-5435.

Thakur, K.G., Joshi, A.M., Gopal, B., 2007. J. Biol. Chem. 282(7), 4711-4718.

Thakur, K.G., Praveena, T., Gopal, B., 2010. J. Mol. Biol. 397(5), 1199-1208.

Tombelli, S., Minunni, M., Mascini, M., 2005. Methods. 37(1), 48-56.

Tsai, T.-T., Shen, S.-W., Cheng, C.-M., Chen, C.-F., 2013. Sci. Technol. Adv. Mate. 14(4), 044404.

tuberculosis Complex, M., 2010. CapiliaTB-Neo.

Tudó, G., Monté, M., Vergara, A., López, A., Hurtado, J., Ferrer-Navarro, M., Vila, J., Gonzalez-Martin, J., 2015. Eur. J. Clin. Microbiol. Infect. Dis. 34(8), 1527-1532.

Upadhyay, P., Hanif, M., Bhaskar, S., 2006. Clin. Microbiol. Infect. 12(11), 1118-1122.

Veigas, B., Fernandes, A.R., Baptista, P.V., 2014. Front Microbiol. 5, 455-455.

Veigas, B., Jacob, J.M., Costa, M.N., Santos, D.S., Viveiros, M., Inácio, J., Martins, R., Barquinha, P., Fortunato, E., Baptista, P.V., 2012. Lab Chip. 12(22), 4802-4808.

Veigas, B., Machado, D., Perdigão, J., Portugal, I., Couto, I., Viveiros, M., Baptista, P.V., 2010. Nanotechnology 21(41), 415101.

Veigas, B., Pedrosa, P., Couto, I., Viveiros, M., Baptista, P.V., 2013. J Nanobiotechnology. 11(1), 1.

Verma, M.S., Rogowski, J.L., Jones, L., Gu, F.X., 2015. Biotechnol. Adv. 33(6), 666-680.

Wang, J., Chen, W.F., Li, Q.X., 2012. Anal. Chim. Acta. 716, 133-137.

Wang, S., Singh, A.K., Senapati, D., Neely, A., Yu, H., Ray, P.C., 2010. Chem. Eur. J. 16(19), 5600-5606.

Wu, Y., Grant, C., 2004. Microweighing in supercritical carbon dioxide. Dekker Encyclopedia of Nanoscience and Nanotechnology, Marcel Dekker, Inc., New York, pp. 1977-1990.

Yang, C., Wang, Y., Marty, J.-L., Yang, X., 2011. Biosens. Bioelectron. 26(5), 2724-2727.

Yang, M., Gao, C., Wang, Y., Zhang, H., He, Z.-G., 2010. PloS one. 5(5), e10672.

Zanchetta, G., Lanfranco, R., Giavazzi, F., Bellini, T., Buscaglia, M., 2017. Nanophotonics. 6(4), 627.

Zeka, A.N., Tasbakan, S., Cavusoglu, C., 2011. J. Clin. Microbiol. 49(12), 4138-4141.

Zhao, W., Chiuman, W., Brook, M.A., Li, Y., 2007. ChemBioChem 8(7), 727-731.

Zhou, L., He, X., He, D., Wang, K., Qin, D., 2011. Clin. Dev. Immunol. 2011.

Table 1. Prominent commercially available molecular methods for TB detection and drug susceptibility testing.

Detection goal	**Type**	**Detection method**	**Commercial test**	**Applied antigen/targeted gene**	**Advantages/disadvantages**	**Turnaround time**	**limit of detection**	**Ref.**
Diagnosing LTBI	TST	DTH measurement	Mantoux test (Pirquet test)	PPD	Widely available, inexpensive, no requirement to special lab infrastructure, False-positive results in BCG-vaccinated	48-72 h	specificity 95%	(Simsek et al. 2010)
			Tine test,	PPD				
			Heaf test (Sterneedle	PPD				

			test)		persons, have reader bias, two patient visit			
	IGRAs	ELISA	QuantiFERON-TB-Gold-In-Tube® (QFT-GIT)	ESAT-6 , CFP-10 & TB7.7 (p4)	Single Patient Visit, Unaffected by BCG, reduction in X-rays radiation, more technically demanding, no reader bias	16-24 h	0.35 IU/ml	(Metcalfe et al. 2013)
		ELISpot	T-SPOT®.TB test	ESAT-6 , CFP-10			specificity ~ 80.9%	(Simsek et al. 2010)
Diagnosing active TB disease and DST	Antigen detection	Immunochromatography	Capilia™ TB-Neo	MPB 64	Simple, consistent with both liquid and solid culture mediums	15 min	1.2×10^6 CFU/mL	(tuberculosis Complex 2010)
		Lateral flow	Alere Determine™ TB LAM Ag	Lipoarabinomannan	Easier sample collection from urine, inexpensive, for HIV positive patients with low CD4 cell count	25 min	sensitivity ~ 95%	(Shah et al. 2016)
	NAATs	Real-time PCR	GeneXpert MTB/RIF	*rpoB*	rapid diagnosis/Higher cost, more technically demanding (excluding Loopamp™)	1h	131 CFU/ml	(Zeka et al. 2011)
		Line probe	INNO-LiPA Rif. TB	*rpoB*		24 h	Not reported	(Pavankumar et al. 2016)
		Line probe	MTBDRplus	*rpoB, katG and inhA*		24 h	160 bacteria/ml	(Pavankumar et al. 2016)
		LAMP	Loopamp™ MTBC Detection Kit	Not reported		40 min	specificity ~ 95.1%	(Nguyen et al. 2018)
		TMA	Gen-Probe Amplified MTD Test	*16s rRNA*		2.5-3.5 h	60 CFU/ml	(Cloud et al. 2004)
		isothermal nucleic acid amplification	EasyNAT® TB Diagnostic Kit	*gyrB*		3 h	sensitivity 19-66.7%, - specificity 100%	(Bholla et al. 2016; Mhimbira et al. 2015)
		Real-time PCR	COBAS® TaqMan® MTB Test	*16s rRNA*		2.5 h	4.0 copies/μl	(Kim et al. 2011)

TST: Tuberculin skin test, IGRAs: Interferon gamma release assays, DTH: delayed-type hypersensitivity, PPD: Purified protein derivatives, NAATs: Nucleic acid amplification tests, LAMP: loop-mediated isothermal amplification, TMA: Transcription mediated amplification, DST: Drug susceptibility testing.

Table 2: Linearity range (LR) and limit of detection (LOD) of some label-free detection systems for diagnosis of *M. tuberculosis*

Detection method	Target	LOD	Linear range	Detection time	Ref.
SPR	CFP-10 antigens	100 ng mL^{-1}	100 ng mL^{-1} - 1μg mL^{-1}	~ 60 min	(Hong et al. 2011a)
	CFP-10 antigens		0.1 - 1 μg mL^{-1}	~ 60 min	(Hong et al. 2011b)
	CFP-10 antigens	as low as 0.1 ng mL^{-1}	0.1 - 150 ng mL^{-1}	80 min	(Chen et al. 2013)
	thiolated single-strand	30 ng μL^{-1}	0.05 μM	20 min	(Duman and

	oligodeoxynucleotide probes (ssODNs)				Piskin 2010)
	IS*6110* and IS*1081* biomarkers	5 fg/μL	5 fg μL^{-1} - 0.5 ng μL^{-1}	18 min for IS6110 21 min for IS1081	(Liu et al. 2018)
	NH_2-end peptide nucleic acid (PNA)	1.0 ng mL^{-1}	Not reported	~ 140 min	(Prabhakar et al. 2008)
	rpoB genes	10 nM	Not reported	120 min	(Rachkov et al. 2011)
Piezoelectric	whole Mtb	2×10^3 cells mL^{-1}	2×10^3 - 3×10^7 cells mL^{-1}	~16 h	(He et al. 2003)
	whole Mtb	10^5 cells mL^{-1}	10^5 cells mL^{-1} - 10^8 cells mL^{-1}	20 min	(He and Zhang 2002)
	IS6110	0.5 μg mL^{-1}	Not reported	20 min	(Kaewphinit et al. 2010a, b)
	whole Mtb and its LAM antigen	8.7×10^5 cells mL^{-1} for α-LAM 8.7×10^6 cells mL^{-1} for anti-H37Rv	Not reported	less than 20 min	(Hiatt and Cliffel 2012)
	whole Mtb	as low as 10 CFU mL^{-1}	10^2 - 10^7 cfu mL^{-1}	24 h	(Ren et al. 2008)
	whole Mtb	10-10^2 CFU mL^{-1}	Not reported	40 h	(Ren et al. 2013)
Gold nanoparticle-based colorimetric approaches	*katG*315 and *rpoB*531 codons	as low as 3 ng of for the *katG* and 30 ng for the *rpoB* gene	Not reported	75 min	(Pavankumar et al. 2016)
	16s rDNA	1 ng for the PCR product and 40 ng for genomic DNA	Not reported	~ 1 h	(Hussain et al. 2013)
	mycobacterial DNA	18.75 ng	Not reported	15 min	(Liandris et al. 2009)
	mycobacterial DNA	Not reported	Not reported	90 min	(Veigas et al. 2013)
	IS6110 dsDNA sequence	2.6 nM	Not reported	~ 1 h	(Tsai et al. 2013)
	mycobacterial DNA	30μg/ml DNA	Not reported	30 min	(Silva et al. 2011)
	CFP-10	10 pg mL^{-1}	10 to 10,000 pg mL^{-1}	10 min	(Kim et al. 2013)
	mycobacterial DNA	10 μg ml^{-1}	10-30 μg ml^{-1}	under 2h30 min	(Veigas et al. 2012)
	mycobacterial DNA	30 ng μL^{-1} of target DNA	Not reported	30 min	(Bernacka-Wojcik et al. 2013)

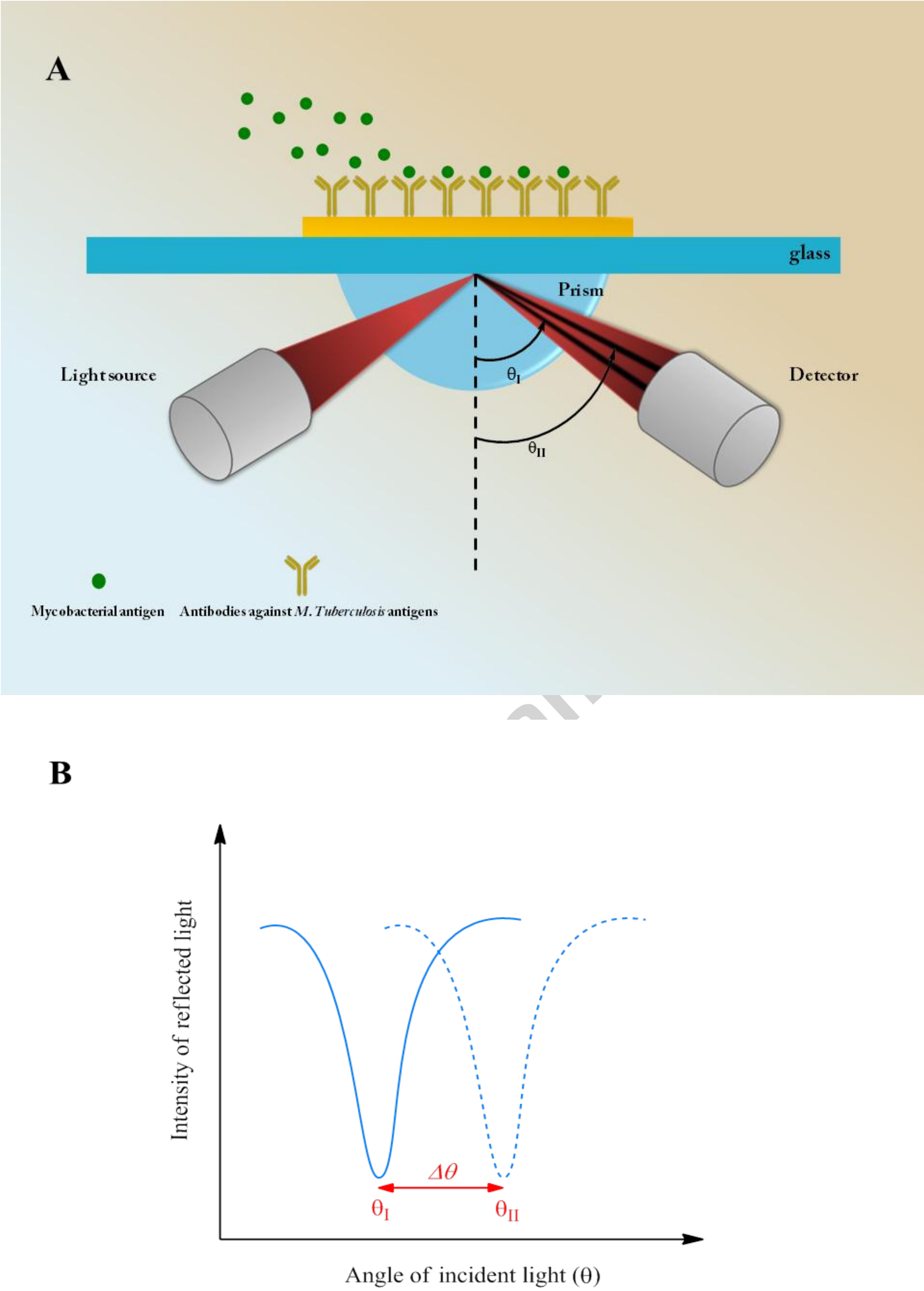
A
glass
Prism
Light source
Detector
θI
θII
Mycobacterial antigen
Antibodies against M. Tuberculosis antigens
B
Intensity of reflected light
Δθ
θI
θII
Angle of incident light (θ)

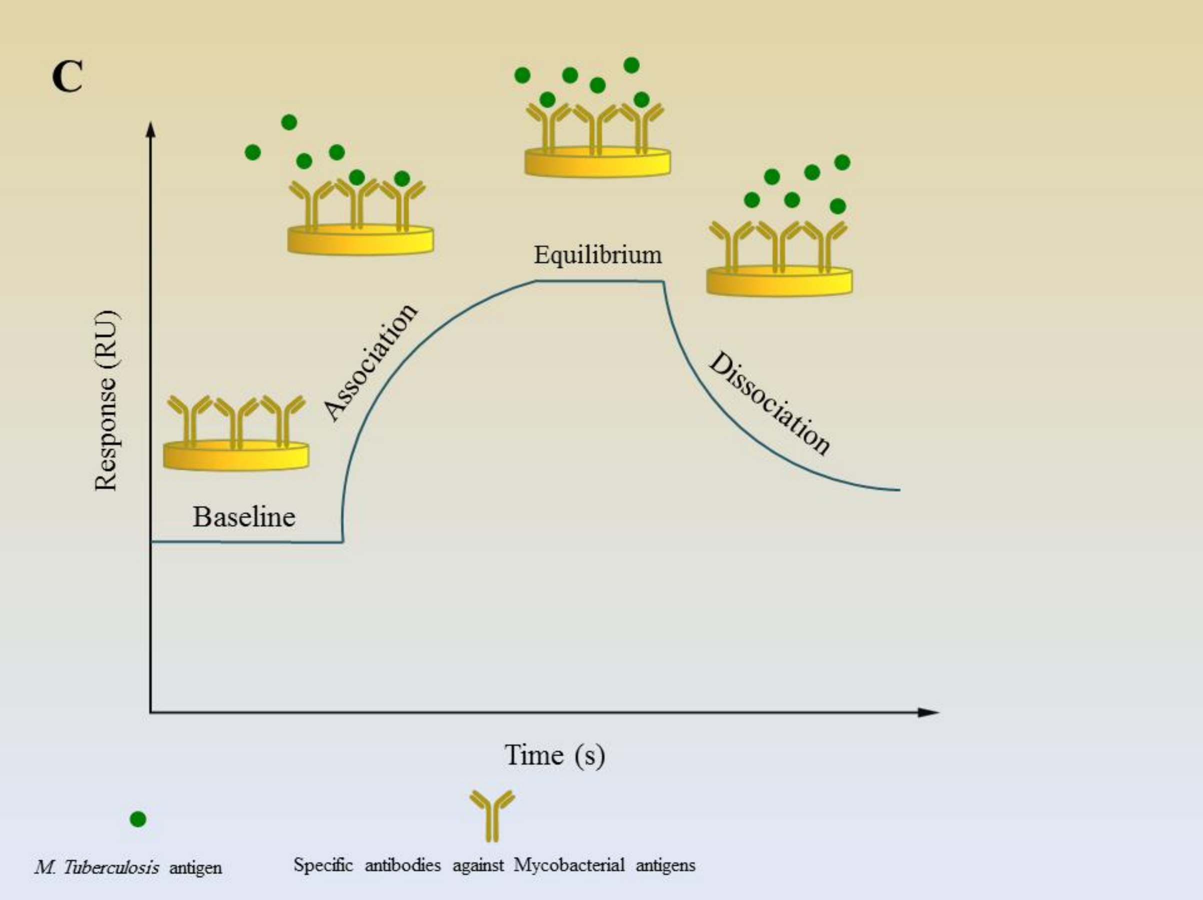

Figure 1. Different scopes of biosensing events occurring during SPR-assisted mycobacterial components sensing. A) General scheme of a SPR system. B) Angle shift that occurs when specific molecules (here, mycobacterial antigens) bind specifically to antibodies attached on thin gold film. C) Kinetic plot of antigen-antibody interaction through SPR-based detection of mycobacterial biomolecules. In the association step, the mycobacterial antigen selectively binds to coated antibodies in which a rise in signal response can be observed. By continuous binding/unbinding of antigens to antibodies, an equilibrium phase is established and appeared as a plateau signal in the plot. Following this steady state, spontaneous unbinding of antigens during dissociation, results in signal loss over time. Reproduced from the references (Daghestani and Day 2010; Nirschl et al. 2011; Sharma et al. 2007).

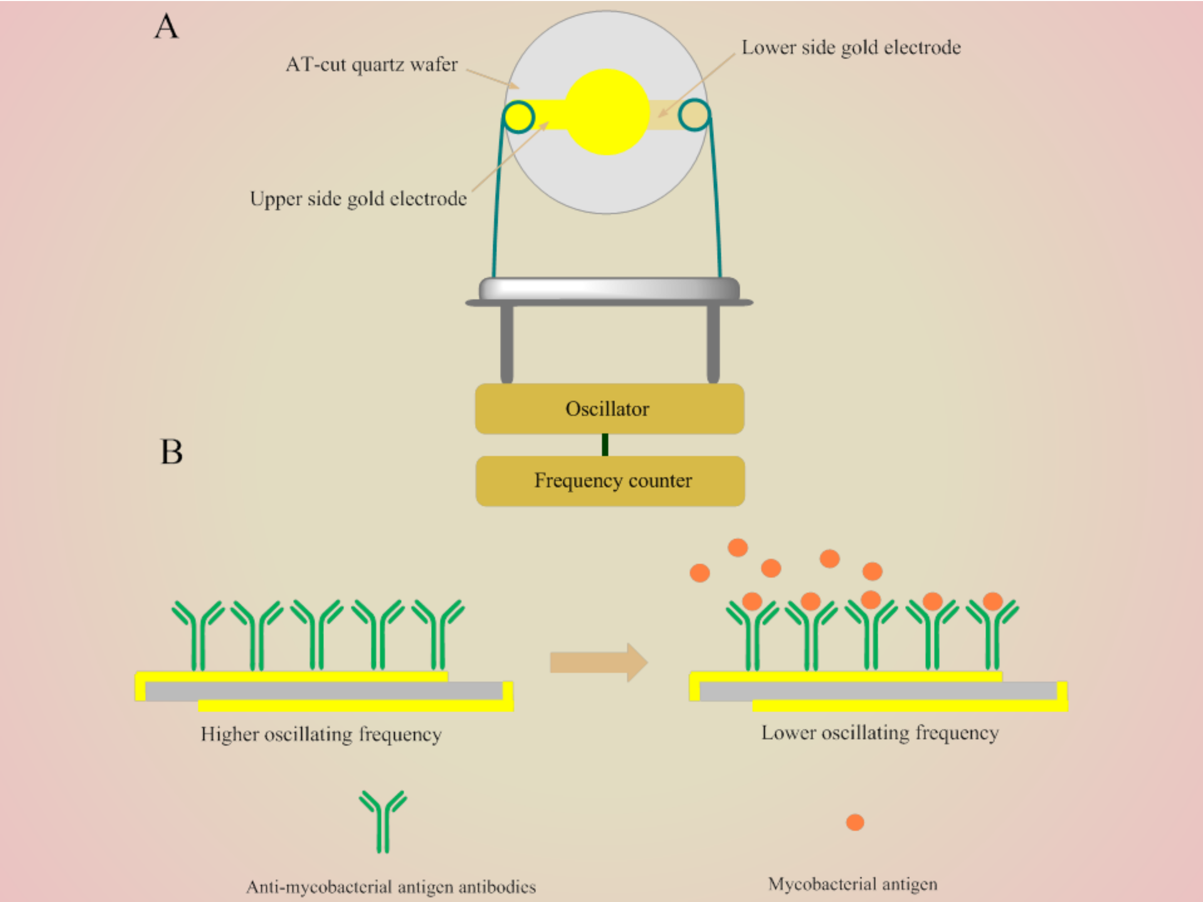

Figure 2. A) Front view of a QCM piezoelectric immunosensor. B) Side view of the immunosensor. Electrical current-induced squeezing of the quartz crystal generates an oscillating frequency. Upon specific binding of antigens with immobilized antibodies, oscillating frequency is reduced enormously. Reproduced from the references (Kumar Singh and Verma 2014; Skládal 2003; Wu and Grant 2004).

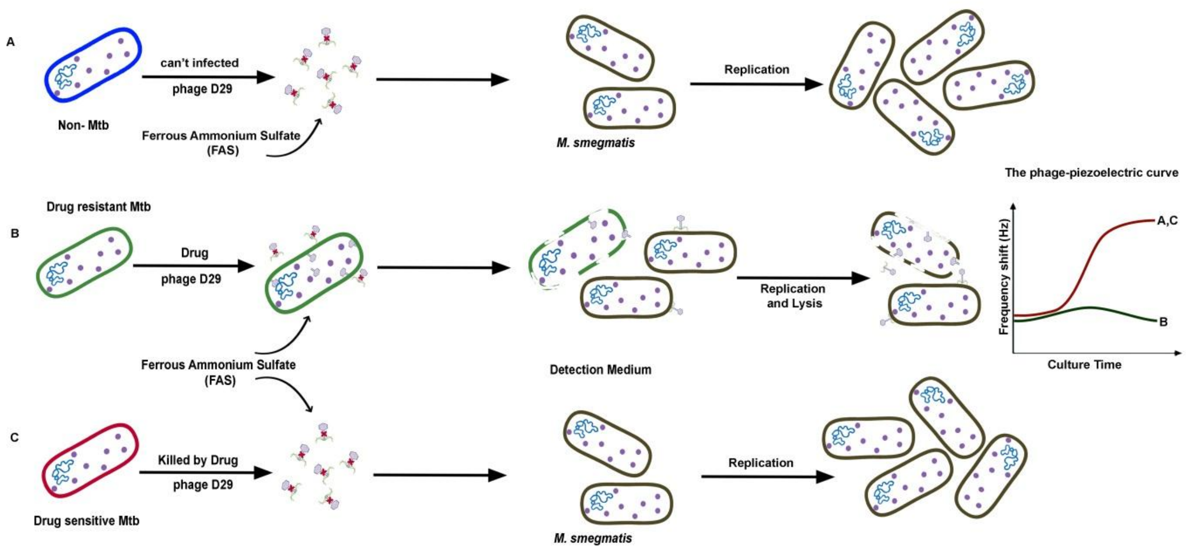

Figure 3. A) In the presence of *Mtb* in medium, its phages are exported to *M. smegmatis* and growth of the latter mycobacterium is restricted. B) Drug resistant strains of *Mtb* remain viable and in the subsequent step, can protect the phage *D29* from inactivation. The protected phages then infect *M. smegmatis*, which finally influences the growth of *M. smegmatis*. C) Drug sensitive strains of *Mtb* are inactivated by drug pretreatment, which therefore cannot protect phages from FAS. Thus, *M. smegmatis* growth is not affected by the phages. Reproduced from the references (Mi et al. 2011, 2014)

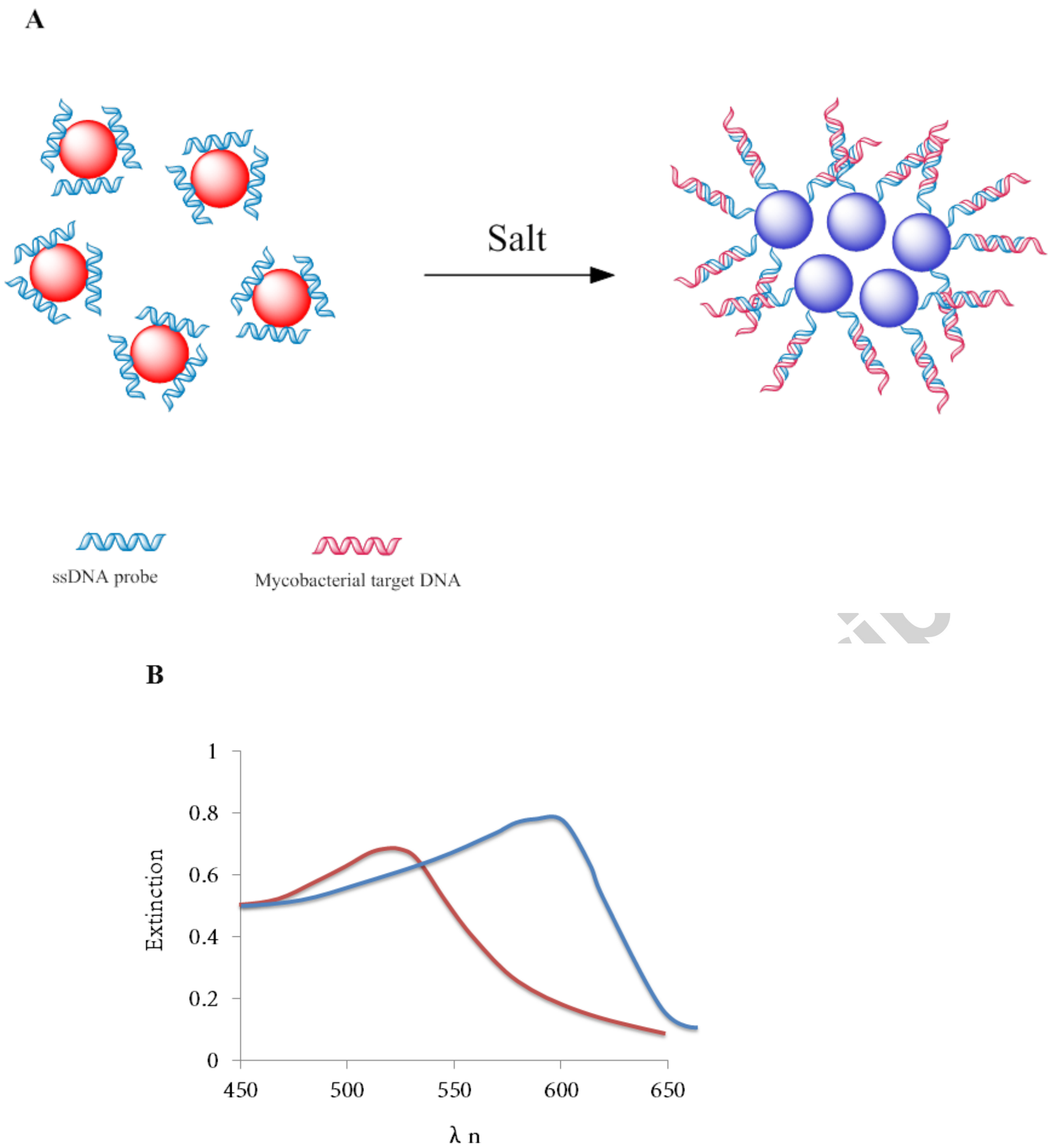

Figure 4. The salt-induced aggregation/dispersion of AuNPs in the colorimetric detection of *Mtb*. A) By adding salt, if the target DNA is present in the medium hybridization occurs and medium color changes to purple. B) A negative response yields a peak around 520 nm (red) while in the presence of the target mycobacterial genomic material this peak shifts to ~600 nm. Reproduced from the references (Veigas et al. 2014; Verma et al. 2015).

highlights

- We review label-free nano-biosensors for tuberculosis detection.
- We provide a focused overview on nano-scale label-free approaches for tuberculosis detection with a detection sensitivity in the femtomolar range for pathogen-raised biomolecules.
- We stress the importance of efficient sensors using low sample volumes as compared to the routine commercialized methods.